Available online at www.sciencedirect.com

ScienceDirect

Energy Procedia 84 (2015) 56 – 61

Energy Procedia

E-MRS Spring Meeting 2015 Symposium C - Advanced inorganic materials and structures for photovoltaics

Preparation and characterization of a-SiC:H absorber layer for semi-transparent solar cells

Y. Vygranenko[a]*, M. Fernandes[a,b], P. Louro [a,b], M. Vieira[a,b], A. Sazonov[c]

[a]CTS-UNINOVA, Quinta da Torre, 2829-516, Caparica, Portugal
[b]Electronics Telecommunications and Computer Engineering, ISEL, Lisbon, 1950-062, Portugal
[c]Electrical and Computer Engineering, University of Waterloo, Waterloo, N2L 3G1, Canada

Abstract

This paper reports on device-quality silicon-carbon alloy (a-SiC:H) application as an absorber material in semi-transparent solar cells. Films with an optical bandgap ranging from 2 to 2.3 eV were prepared by plasma enhanced chemical vapour deposition (PECVD). The n-i-p structures with undoped SiC:H layers deposited under the same experimental conditions were also fabricated and characterized. The optimized devices showed forward current-voltage characteristics with a diode ideality factor in the range from 1.4 to 1.8, and an open circuit voltage up to 0.92V. The density of deep defect states in a SiC:H was estimated from the transient current measurements and correlated with the optical bandgap.

© 2015 Published by Elsevier Ltd. This is an open access article under the CC BY-NC-ND license
(http://creativecommons.org/licenses/by-nc-nd/4.0/).

Peer-review under responsibility of The European Materials Research Society (E-MRS)
Keywords: amorhous silicon-carbon alloy; thin-film solar cells; density of states.

1. Introduction

Semi-transparent thin-film solar cells have great potential for residential and office building installations as they can be easily incorporated in a typical window to generate electricity and yet allow daylight for tenant's visual comfort [1,2]. Although full-penetration a-Si:H-based solar cells have been studied for application to PV windows owing to their large area deposition capability, low production cost and high reliability, the remaining issue is that

* Corresponding author. Tel.: +351-21-831-7287; fax: +351-21-831-7114.
E-mail address: yvygranenko@deetc.isel.ipl.pt

1876-6102 © 2015 Published by Elsevier Ltd. This is an open access article under the CC BY-NC-ND license
(http://creativecommons.org/licenses/by-nc-nd/4.0/).

Peer-review under responsibility of The European Materials Research Society (E-MRS)
doi:10.1016/j.egypro.2015.12.295

their power conversion efficiency, transparency and colour cannot be controlled independently [3]. a-Si:H-carbon alloys allow to wider the optical gap and to vary the refractive index of the material thus giving more flexibility in controlling optical and photovoltaic device characteristics [4]. However, the use of undoped a-SiC:H as an active layer material is limited by its high defect density. Several research groups have demonstrated that the hydrogen dilution of source gas mixture can reduce both defect density and disorder in the a-SiC:H films made by plasma enhanced chemical vapour deposition (PECVD) [5-8].

Two distinct deposition regimes are observed for a-SiC:H films grown in silane-methane discharge as a function of RF power [9]. In the low-power regime, the RF power density delivered to plasma is below the threshold of CH_4 primary decomposition and carbon incorporation comes from chemical reaction between CH_4 molecules and the radicals produced by SiH_4 decomposition. In this mode, the carbon is incorporated mainly in methyl groups (-CH_3) thus preserving the sp^3 hybridization in the solid. The properties of a "chemically ordered" alloy depend only weakly on the deposition parameters other than the gas mixture [10]. In the high-power regime, both SiH_4 and CH_4 are subject to primary decomposition thus enhancing the carbon incorporation efficiency. C-rich films with a defect density lower than 2×10^{17} cm^{-3} deposited in high power regime at high H-dilution have been reported elsewhere [11].

In this paper, we report on the performance of the n–i–p structures with an a-SiC:H absorber layer deposited in hydrogen diluted silane-methane plasma under low-power regime. The optical bandgap of undoped a-SiC:H was varied by adjusting the RF power, and the electronic properties were obtained from current-voltage and transient current measurements.

2. Experimental

2.1. Film and device deposition

The films and n-i-p structures for this study were prepared at 200 °C using a multichamber 13.56 MHz PECVD system, manufactured by MVSystems Inc. The a-SiC:H films for electrical and optical characterization were deposited onto Corning 1737 glass substrates using a (SiH_4 + CH_4 + H_2) gas mixture with the ratio of 1:1:20 at the pressure of 1 Torr. The RF power was varied from 5 to 80 W corresponding to the power density in the range from 23 to 364 mW/cm^2.

The a-SiC:H n-i-p cells were fabricated by the following deposition sequence. First, ~100 nm thick Mo film was sputtered on the glass substrate, followed by the deposition of the n-i-p stack. Finally, 65 nm thick ITO film was sputtered and patterned to form the top electrodes with area ranging from 1 × 1 to 5 × 5 mm^2.

The trimethylboron ($B(CH_3)_3$) (TMB) and phosphine (PH_3), diluted in hydrogen to concentration of 1%, were used as the doping gases. The 20 nm thick doped films were deposited at CH_4/SiH_4 flow rate ratio of 1, and TMB/SiH_4 or PH_3/SiH_4 ratio of 0.01. The pressure and RF power were 600 mTorr and 4 W, respectively. A number of the n-i-p structures was deposited under different RF power conditions for the a-SiC:H i-layer. Other deposition parameters were kept constant as described above for all films. An a-Si:H n-i-p structure with a-SiC:H p-layer was also fabricated and used as a reference sample in the test experiments. The i-layer was deposited using (SiH_4 + H_2) gas mixture with the ratio of 1:3 at the pressure of 600 mTorr.

2.2. Characterization techniques

The transmission and reflection spectra of a-SiC:H films were measured using UV-visible 2501PC Shimadzu spectrophotometer. The optical bandgap was obtained from the absorption coefficient α versus energy plot as the energy E_{04} at which α was equal to 10^4 cm^{-1}. Note that in the case of silicon-carbon alloys, it is difficult to define the optical bandgap using Tauc procedure because the $(\alpha h\nu)^{1/2}$ vs energy ($h\nu$) plot does not show a linear trend. The E_{04} gap is an easy-to-obtain parameter, which is conventionally used for amorphous materials.

For transient current measurements, special setup was assembled whose block diagram is shown in Fig. 1(a). It includes charge amplifier, two pulse generators, digital oscilloscope, and personal computer (PC) with GPIB card and custom software. The first pulse generator provides bias pulses to the diode structure under test, triggering pulses to the digital oscilloscope and the second pulse generator. The second pulse generator controls a reset switch

of the charge amplifier. The digital oscilloscope captures the output signal of the charge amplifier, and saves acquired waveforms in the computer. The timing and biasing scheme is shown in Fig. 1(b). During the time interval T_f, a forward current pulse is applied to the diode thus limiting the injected charge. The current pulse amplitude, $I_f = (V_f–V_d)/R$, is varied by adjusting V_f or the resistor R. The value of V_f is chosen to be several times larger than the voltage drop across the diode, V_d. After the trap-filling pulse, the diode is reverse biased with a voltage V_r. The switch S_1 is open-circuited with a small delay, t_1, to avoid the initial current transient related to the sample capacitance, and the input current is integrated by capacitor C_f, resulting in the observed variation of the output voltage. To reduce the noise level, the output waveforms were captured by a digital oscilloscope in averaging mode with 128 readings. Time dependence of input current ($I_{inp}(t)$) was obtained by transforming the output waveform $V_{out}(t)$ according to the equation

$$I_{inp} = C_f \cdot \frac{dV_{out}}{dt}, \tag{1}$$

where C_f is the feedback capacitor of the charge amplifier. Feedback capacitor of C_f=1 nF was used for testing 2×2 mm^2 n-i-p structures.

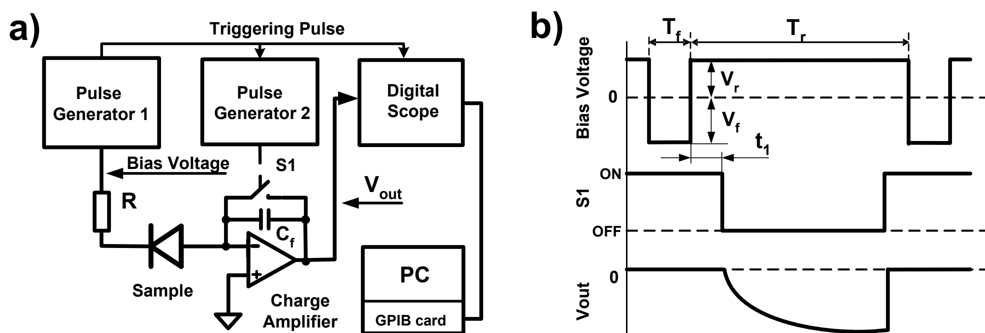

Fig. 1. (a) Block diagram of the transient current measurement setup and (b) signal waveforms.

3. Results and discussion

Fig. 2 shows the deposition rate and optical bandgap (E_{04}) as a function of RF power (P_{rf}). The deposition rate is found to be proportional to $log(P_{rf})$ in the range from 5 to 80 W. The increase in E_{04} with increasing P_{rf} follows the same dependence in the range 10 to 80 W. The dark conductivity of the films decreases with increasing P_{rf} in the

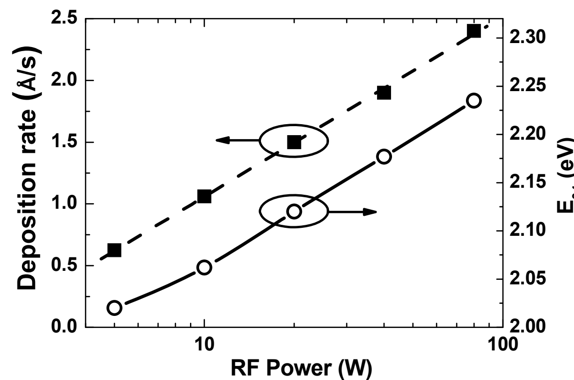

Fig. 2. Deposition rate and optical bandgap of the a-SiC:H films as a function of RF power coupled to the plasma.

range from 8×10^{-9} down to 1.1×10^{-11} S/cm. It can be concluded that the increase in RF power leads to an enhancement of the carbon incorporation thus widening the bandgap and decreasing the dark conductivity.

Fig. 3 shows the typical quasi-static current-voltage (*J-V*) characteristics of a-SiC:H n-i-p structures with *i*-layers deposited at RF power of 5, 10, 20, and 40 W, respectively. The *J-V* curve of a-Si:H n-i-p diode (sample #5) is also shown for comparison. In order to minimize the transient current induced by the trapped charge in the *i*-layer, the sweep delay was set to 20 s and the bias voltage was varied with 25 mV increments.

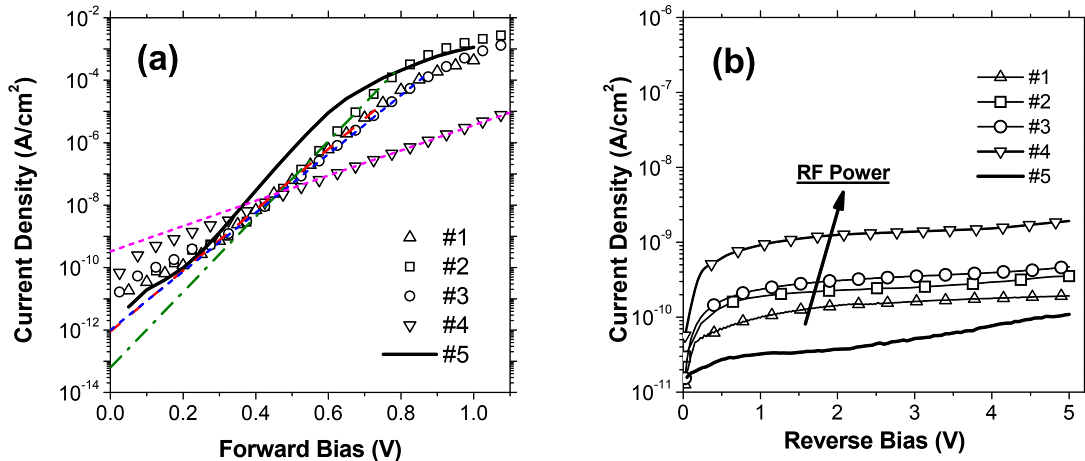

Fig. 3. Current-voltage characteristics of *n-i-p* diodes under (a) forward bias and (b) reverse bias.

Saturation current density (J_o), and diode ideality factor (n) deduced from I-V curves are shown in Table 1 along with deposition parameters (RF power, optical bandgap (E_{04}), *i*-layer thickness). The open circuit voltage (V_{oc}) measured under 1.5AM illumination conditions is also presented in Table 1.

Samples #1, #2, and #3 show an exponential dependence of the forward current over five orders of magnitude in the biasing range from 0.2 to 0.75 V. Sample #2 (P_{rf} = 10W) yields the lowest J_o and n of all a-SiC:H n-i-p diodes (63 fA/cm^2 and 1.43, respectively). Furthermore, sample #4 has the widest optical bandgap (E_{04} = 2.18 eV) and shows different performance yielding J_o= 390 pA/cm^2 and n = 4.27. Different mechanisms can be responsible for poor device performance. As the carbon content in a-SiC:H increases, the mobility-lifetime product drops exponentially, what could lead to enhanced recombination under forward bias [6,12]. On the other side, at high RF power, the admixture of sp^2 bonds may also worsen the electronic properties of the material. Further research is needed to clarify the mechanism of this change.

For a-SiC:H n-i-p structures, the V_{oc} values are in the range from 0.861 V to 0.918 V. Similar values have been reported elsewhere [13] for solar cells with VHF PECVD deposited a-SiC:H absorber. As expected, an increase in V_{oc} with increasing E_{04} is observed for samples #1 and #3, which have similar values of J_o and n. Sample #2 shows lower Voc than that of sample #1 even at higher E_{04} because of higher forward dark current due to lower n.

In Fig. 3(b), one can see that the current density under reverse bias increases at higher RF power. For example, the dark current density is ranging from 190 pA/cm2 to 2 nA/cm^2 at reverse bias of 5 V. The lowest leakage current

Table 1. RF power, optical bandgap (E_{04}), *i*-layer thickness, saturation current density (J_o), diode ideality factor (n), and open circuit voltage (V_{oc}) of the fabricated *n-i-p* structures.

Sample (N^o)	RF Power (W)	E_{04} (eV)	*i*-layer thickness (nm)	J_0 (pA/cm^2)	n	V_{oc} (V)
#1	5	2.02	250	0.9	1.76	0.880
#2	10	2.06	210	0.063	1.43	0.861
#3	20	2.12	320	1	1.82	0.918
#4	40	2.18	580	390	4.27	0.885
#5	5	1.88	490	0.22	1.33	0.819

is observed in the reference sample (sample #5). Here, the dark current density of 100 pA/cm^2 is comparable to that reported for state-of-the-art a-Si:H photodiodes [14]. The leakage current in the sample #1 is only a factor of 3 higher than that for the reference a-Si:H sample, suggesting low defect density in optimized a-SiC:H films. Thermal generation of charge carriers via midgap defects states in the *i*-layer is likely the main source of leakage in samples #1 to #3. The defect density in a-$Si_{1-x}C_x$:H increases with increasing RF power thus leading to higher leakage current.

Transient dark current measurements were performed to estimate the density of states in the *i*-layer bulk. After trap-filling forward current pulse, current transients associated with thermal emission of trapped carriers were measured within time range from 10 to 500 ms. Our method is similar to the measurements and analysis of photocurrent transients in a-Si:H photodiodes reported in Ref. 15. Durations of biasing pulses T_f and T_r were 5 and 495 ms, respectively (see Fig.1 b). The forward current density of the trap-filling pulse was kept constant at 680 µA/cm^2, and the transient current was measured at V_r=2 V. The transient current observed follows power law time dependency given by,

$$I_{dark}(t) = \Delta I(t_0)(t_0/t)^{\beta}, \tag{2}$$

where $\Delta I(t_0)$ is the transient current at time t_0, and β is dimensionless constant. β was determined to be 0.88-0.91 for our a-SiC:H diodes. The emission rate of trapped charge can then be calculated from the transient dark current according to

$$G(t) = \frac{I_{dark}(t)}{qAd_i}, \tag{3}$$

where q is the elementary charge, A the diode area, and d_i the *i*-layer thickness. Fig. 4 shows *log-log* plot of $G(t)$ for our samples. As can be seen here, the emission rate magnitude for a-SiC:H samples increases with RF power, exceeding the one for the reference sample by 4.6 to 8.3 times at t=0.3 s. Assuming midgap defect density (N_d) of 10^{16} cm^{-3}eV^{-1} for the reference a-Si:H diode, which is consistent with its leakage current, the values for tested a-SiC:H samples can be obtained. Inset in Fig. 4 shows that the relation between N_d and E_{04} is close to linear. The increase in N_d can be attributed to carbon incorporation, and to defects induced by increasing ion bombardment of film surface. The C-induced defects are most likely dominant because, as observed, both N_d and E_{04} are found to be proportional to carbon concentration.

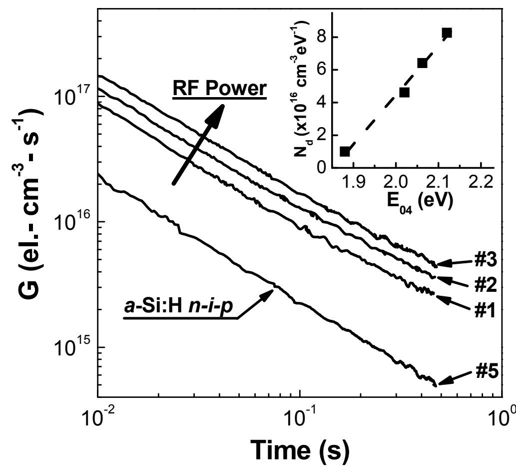

Fig. 4. Emission rate of trapped charge in reverse biased *n-i-p* structure after applying a trap-filling forward current pulse of 680 µA/cm^2. Density of deep defect states versus the optical bandgap plot is shown in the inset.

4. Conclusion

In this study we have shown that the deposition rate, dark conductivity and optical bandgap in the a-SiC:H films grown by PECVD can be varied by adjusting the RF power coupled to the plasma. The fabricated n-i-p structures with an a-SiC:H absorber layer have optical bandgap E_{04} ranging from 2 to 2.12 eV and show low (<500 pA/cm^2) reverse dark current density. The achieved diode ideality factor is in the range from 1.4 to 1.8, and the open circuit voltage is up to 0.92 V. The midgap defect density in optimized a-SiC:H is estimated to be (4–8) × 10^{16} cm^{-3}-eV^{-1}. From the experiment, one can conclude that device-quality a-SiC:H films can be grown in the low power regime at substrate temperature of 200°C.

Acknowledgements

The authors are grateful to the Portuguese Foundation of Science and Technology through fellowship SFRH/BPD/102217/2014 and to Natural Science and Engineering Research Council (NSERC) of Canada for financial support of this research.

References

[1] K. Kapsis, Andreas K. Athienitis. A study of the potential benefits of semi-transparent photovoltaics in commercial buildings. Solar Energy 2015; 115: 120–132.
[2] Y.T. Chae et al. Building energy performance evaluation of building integrated photovoltaic (BIPV) window with semi-transparent solar cells. Applied Energy 2014; 129: 217–227.
[3] S.H. Lee, S. J. Yun, M. Shin, and J. W. Lim. Cu_2O thin films as the color-adjusting layer in semi-transparent a-Si:H solar cells. Solar Energy Materials&SolarCells 2013;117:519–525.
[4] R. Gharbi, M. Fathallah, C.F. Pirri, E. Tresso, G. Crovini, and F. Giorgis. Properties of a-SiC:H films and solar cells. Can. J. Phys. 1999; 77: 699–704.
[5] A. Matsuda, T. Yamaoka, S. Wolff, M. Koyama, Y. Imanishi, H. Kataoka, H. Matsuura and K. Tanaka. Preparation of highly photosensitive hydrogenated amorphous Si-C alloys from a glow-discharge plasma. J. Appl. Phys. 1986; 60: 4025-4027.
[6] A. Desalvo, F. Giorgis, C. F. Pirria, E. Tresso, P. Rava, R. Galloni, R. Rizzoli, and C. Summonte. Optoelectronic properties, structure and composition of a-SiC:H films grown in undiluted and H_2 diluted silane-methane plasma. J. Appl. Phys. 1997; 81: 7973-7980.
[7] F. Demichelis, G. Crovini, C.F. Pirri, E. Tresso, R. Galloni, R. Rizzoli, C. Summonte, F. Zignani, P. Rava, and A. Madan. The influence of hydrogen dilution on the optoelectronic and structural properties of hydrogenated amorphous silicon carbide film. Phil. Mag. B 1994; 69 : 377-386.
[8] C. Gemmer, Markus B. Schubert. Device Quality Silicon Carbon Thin Films. Mater. Res. Soc. Symp. Proc. 2000; 609: A23-03.
[9] I. Solomon. Amorphous silicon–carbon alloys: a promising but complex and very diversified series of materials. Appl. Surf. Sci. 2001; 184: 3-7.
[10] P. Rava, G. Grovini, F. Demichelis, F. Giogis, and C.F. Pirri. Characterization of the effect of growth conditions on a-SiC films. J. Appl. Phys. 1996; 80: 4116.
[11] G. Ambrosone, V. Ballarini , U. Coscia, S. Ferrero, F. Giorgis, P. Maddalena, A. Patelli, P. Ravac, and V. Rigato. Properties of a-SiC:H films deposited in high power regime. Thin Solid Films 2003; 427: 279-283.
[12] J. P. Conde, V. Chu, M. F. da Silva, A. Kling, Z. Dai, J. C. Soares, S. Arekat, A. Fedorov, M. N. Berberan-Santos, F. Giorgis and C. F. Pirri. Optoelectronic and structural properties of amorphous silicon–carbon alloys deposited by low-power electron-cyclotron resonance plasma-enhanced chemical-vapor deposition. J. Appl. Phys. 1999; 85(6): 3327.
[13] R. Platz, D. Fischer, A. Shah. VHF-deposited a-SiC:H alloys for high-bandgap solar cells. Mater. Res. Soc. Symp. Proc. 1995; 377: 645-651.
[14] J.A. Theil. Leakage current behavior in common i-layer a-Si:H p-i-n photodiode arrays. Mater. Res. Soc. Symp. Proc. 2003, 762: A.21.4.1.
[15] H. Nozaki, T. Kamimura, N. Sakuma, and H. Ito. Measurement and analysis of photocurrent transient characteristics for hydrogenated amorphous-silicon photodiodes. IEEE Trans. Electron. Devices 1989; 36: 2810 - 2815.